Supporting Information for:

Spin-state dependence of the structural and vibrational properties of solvated iron(II) polypyridyl complexes from AIMD simulations: III. [Fe(tpen)]Cl_2 in acetonitrile

Latévi M. Lawson Daku

Département de chimie physique, Université de Genève, Quai E. Ansermet 30, CH-1211
Genève 4, Switzerland. E-mail: max.lawson@unige.ch

Contents

1 Structural properties of the solution **4**

1.1 LS and HS structures of $[Fe(tpen)]^{2+}$ 4

1.2 Inner solvation shell of HS $[Fe(tpen)]^{2+}$ 7

1.3 Structure of the acetonitrile solvent for $[Fe(tpen)]^{2+}$ in the LS and HS states 8

1.4 Solvation structure of Cl^- 10

2 Vibrational properties **12**

2.1 Calculated 310 K Infrared spectrum of the acetotrinile solvent 12

2.2 Infrared spectra $[Fe(tpen)]^{2+}$ in the LS and HS states 12

List of Figures

S1 Distribution function of the angles Π_1 and Π_2 4

S2 Distribution functions of the Fe-$C_i \equiv$ Fe-C'_i ($i = 1, \ldots, 7$) distances 5

S3 Distribution functions of the Fe-C_ζ ($\zeta = \beta, \gamma, \delta$) distances 6

S4 Snapshots from the HS trajectory showing the acetonitrile molecule(s) in the inner solvation shell of HS $[Fe(tpen)]^{2+}$ 7

S5 Structure of the acetonitrile solvent for $[Fe(tpen)]^{2+}$ in the LS state 8

S6 Structure of the acetonitrile solvent for $[Fe(tpen)]^{2+}$ in the HS state 9

S7 Solvation structure of Cl^- for $[Fe(tpen)]^{2+}$ in the LS (Top) and in the HS state (Bottom): radial distribution functions $g(r)$ of the acetonitrile nitrogen (N_{ACN}), carbon ($N_{ACN}{\equiv}C^1_{ACN}{-}C^2_{ACN}$) and hydrogen ($H_{ACN}$) atoms with respect to the Cl atom (solid lines, left y-axis), and running coordination numbers $cn(r)$ (dashed lines, left y-axis). 10

S8 Snapshot from the LS trajectory illustrating the first solvation shell of the Cl^- counterions 11

S9 Time dependence of the Fe-Cl distances for $[Fe(tpen)]^{2+}$ in the LS and HS states 11

S10 Calculated 310 K IR spectra of acetonitrile for $[Fe(tpen)]^{2+}$ in the LS and HS state. 12

S11 Calculated 310 K IR spectra of $[Fe(tpen)]Cl_2$ and $[Fe(tpen)]^{2+}$ in acetonitrile 13

1 Structural properties of the solution

1.1 LS and HS structures of $[\mathrm{Fe(tpen)}]^{2+}$

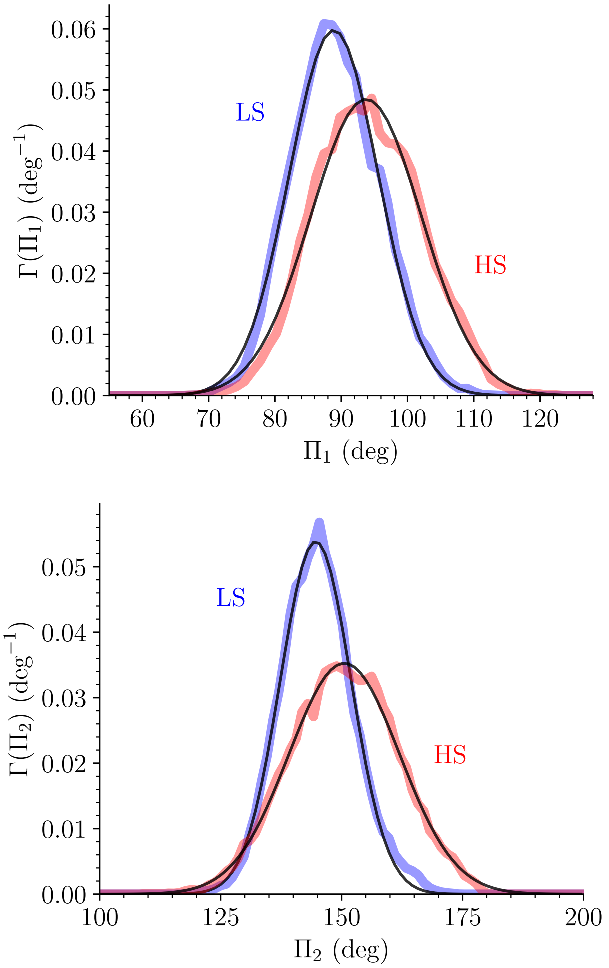

Figure S1 Distribution functions of the angles Π_1 (Top) between the three-atom planes $\mathcal{P}(\mathrm{C}_6, \mathrm{N}_3, \mathrm{C}_7)$ and $\mathcal{P}(\mathrm{C}'_6, \mathrm{N}'_3, \mathrm{C}'_7)$ and of the plane Π_2 (Bottom) between the three-atom planes $\mathcal{P}(\mathrm{C}_3, \mathrm{N}_2, \mathrm{C}_4)$ and $\mathcal{P}(\mathrm{C}'_3, \mathrm{N}'_2, \mathrm{C}'_4)$ for $[\mathrm{Fe(tpen)}]^{2+}$ in acetonitrile and in the LS and HS states. The fits of the data with Gaussian distribution functions are also shown (black lines).

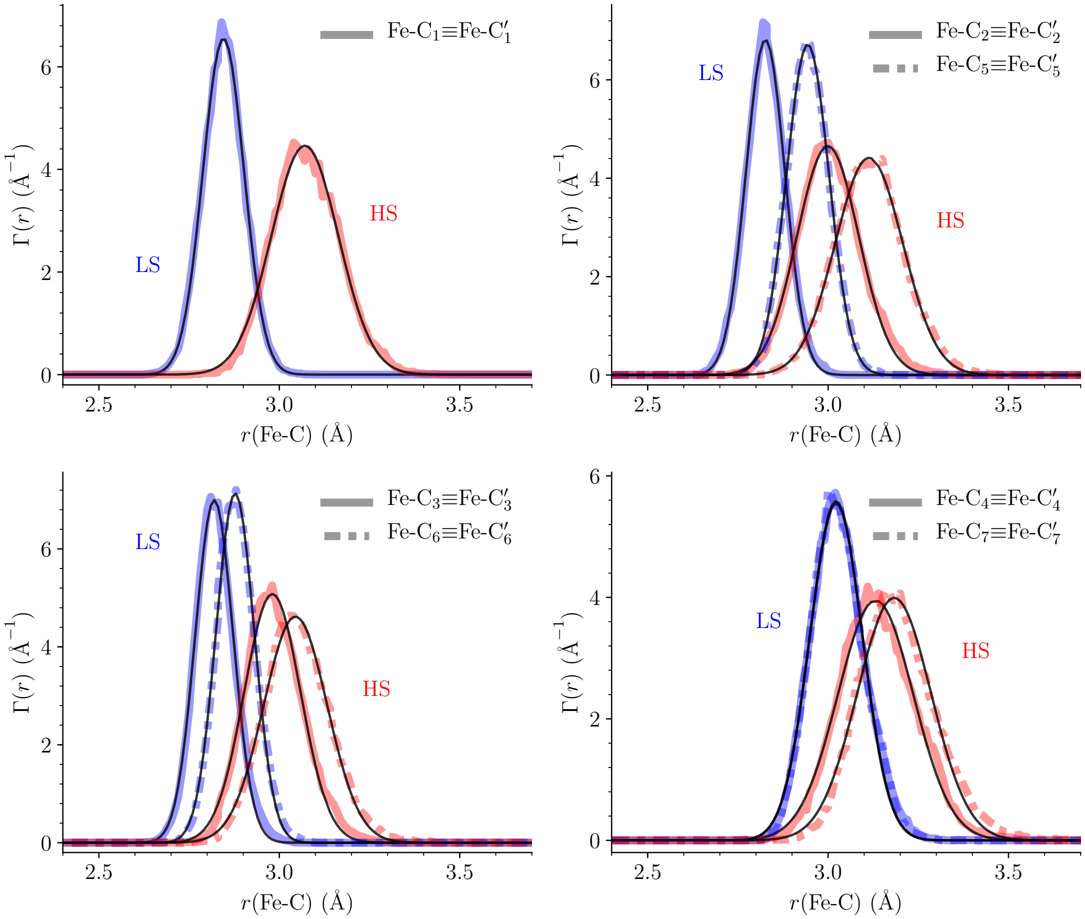

Figure S2 Distribution functions of the Fe-C$_i$ $\equiv$ Fe-C$'_i$ ($i = 1, \ldots, 7$) distances for [Fe(tpen)]$^{2+}$ in acetonitrile and in the LS and HS states (thick solid or dashed lines). The fits of the data with Gaussian distribution functions are also shown (black lines).

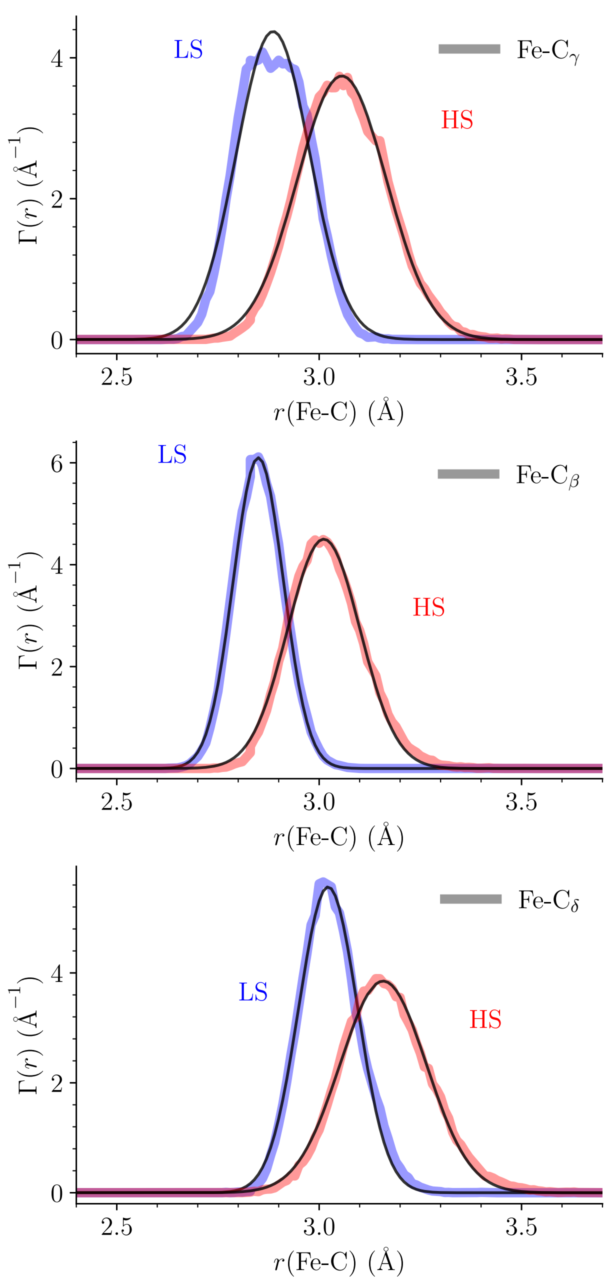

Figure S3 Distribution functions of the Fe-C_ζ ($\zeta = \beta, \gamma, \delta$) distances for $[\mathrm{Fe(tpen)}]^{2+}$ in acetonitrile and in the LS and HS states (thick solid lines). C_β designates the carbon atoms C_i and C'_i ($i = 3, 6$), C_γ the carbon atoms C_i and C'_i ($i = 2, 5$), and C_δ the atoms C_i and C'_i ($i = 4, 7$). The fits of the data with Gaussian distribution functions are also shown (black lines).

1.2 Inner solvation shell of HS $[Fe(tpen)]^{2+}$

Figure S4 shows snapshots from the HS trajectory illustrating the presence of ACN molecules in the inner solvation shell of HS $[Fe(tpen)]^{2+}$.

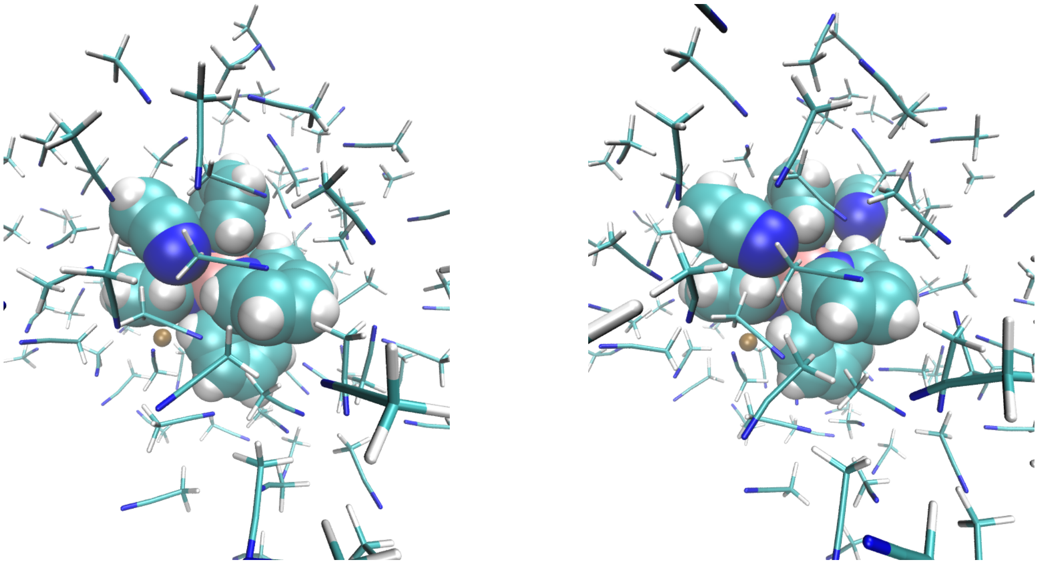

$t = 30162.5$ fs

$t = 31650.0$ fs

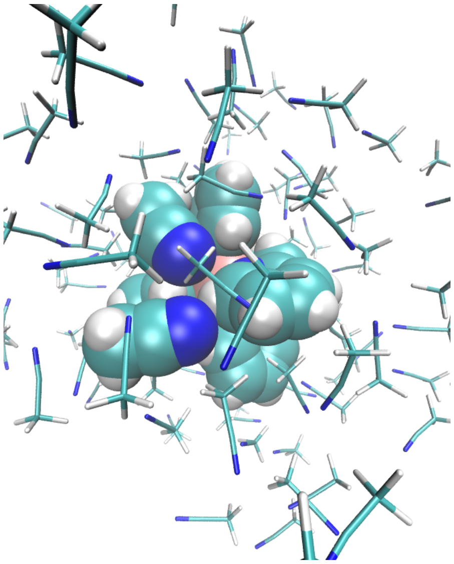

$t = 39972.5$ fs

Figure S4 Snapshots from the HS trajectory showing the acetonitrile molecule(s) in the inner solvation shell of HS $[Fe(tpen)]^{2+}$ at different timesteps: the complex and the acetonitrile molecule(s) in its inner solvation shell are drawn with a van der Waals representation, the other acetonitrile molecules with a licorice representation, and the Cl^- anions with a CPK representation.

1.3 Structure of the acetonitrile solvent for $[\mathrm{Fe(tpen)}]^{2+}$ in the LS and HS states

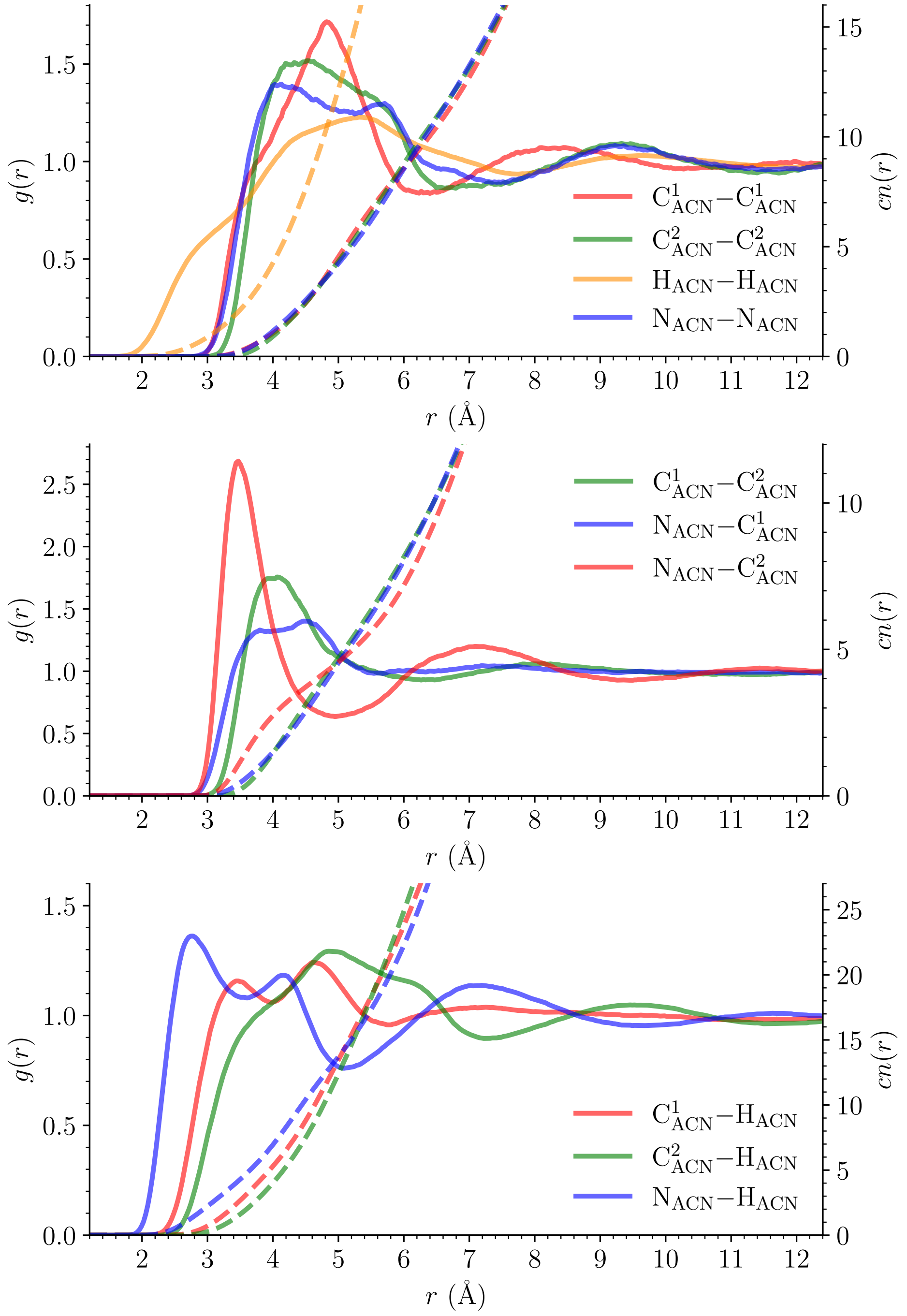

Figure S5 Structure of the acetonitrile solvent for $[\mathrm{Fe(tpen)}]^{2+}$ in the LS state (atom labeling: $\mathrm{N_{ACN}{\equiv}C^1_{ACN}{-}C^2_{ACN}\,(H_{ACN})_3}$): intermolecular radial distribution functions $g(r)$ (solid lines, left y-axis) and running coordination numbers $cn(r)$ (dashed lines, left y-axis).

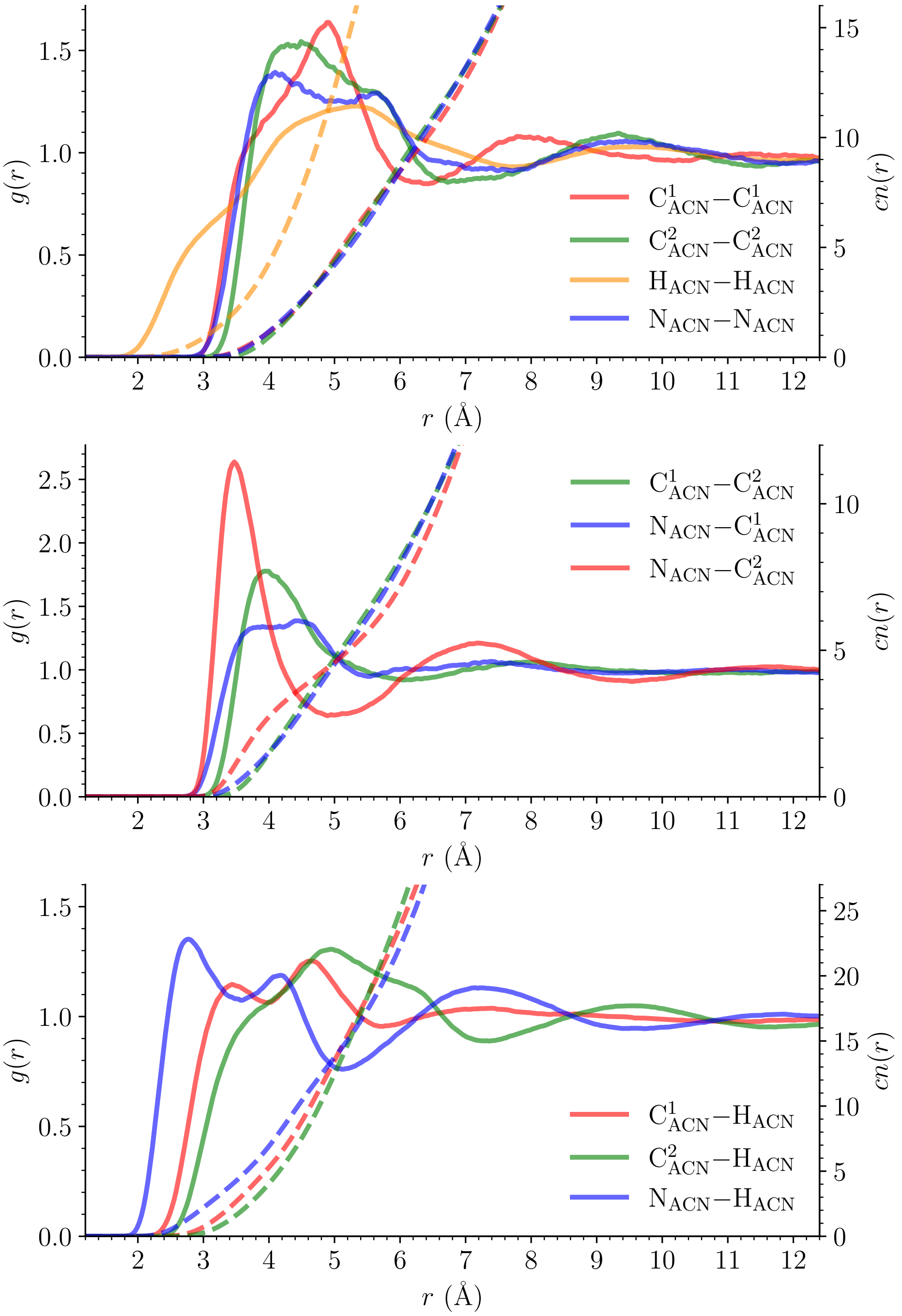

Figure S6 Structure of the acetonitrile solvent for $[\mathrm{Fe(tpen)}]^{2+}$ in the HS state (atom labeling: $\mathrm{N_{ACN}{\equiv}C^1_{ACN}{-}C^2_{ACN}\,(H_{ACN})_3}$): intermolecular radial distribution functions $g(r)$ (solid lines, left y-axis) and running coordination numbers $cn(r)$ (dashed lines, left y-axis).

1.4 Solvation structure of Cl^-

Figure S7 shows the Cl-ACN radial distribution functions (RDFs) and the associated running coordinations numbers characterizing the solvation structure of the Cl^- anions for $[Fe(tpen)]^{2+}$ in the LS and HS states.

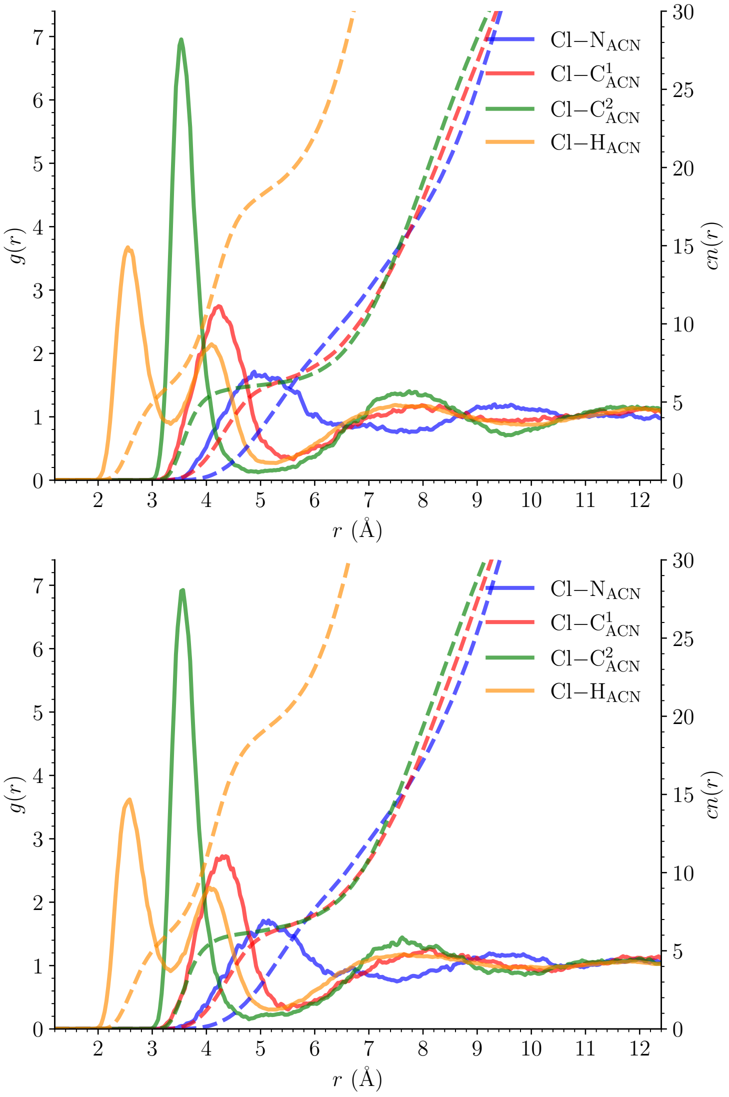

Figure S7 Solvation structure of Cl^- for $[Fe(tpen)]^{2+}$ in the LS (Top) and in the HS state (Bottom): radial distribution functions $g(r)$ of the acetonitrile nitrogen (N_{ACN}), carbon ($N_{ACN} \equiv C^1_{ACN} - C^2_{ACN}$) and hydrogen ($H_{ACN}$) atoms with respect to the Cl atom (solid lines, left y-axis), and running coordination numbers $cn(r)$ (dashed lines, left y-axis).

Figure S8 shows snapshots from the LS trajectory which illustrate the first solvation shell of the Cl^- counterions. During the AIMD simulations, the anions are found to stay in the vicinity of [Fe(tpen)]$^{2+}$, as shown by the plot in S9 of the time dependence of the Fe-Cl distances for [Fe(tpen)]$^{2+}$ in the LS and HS states.

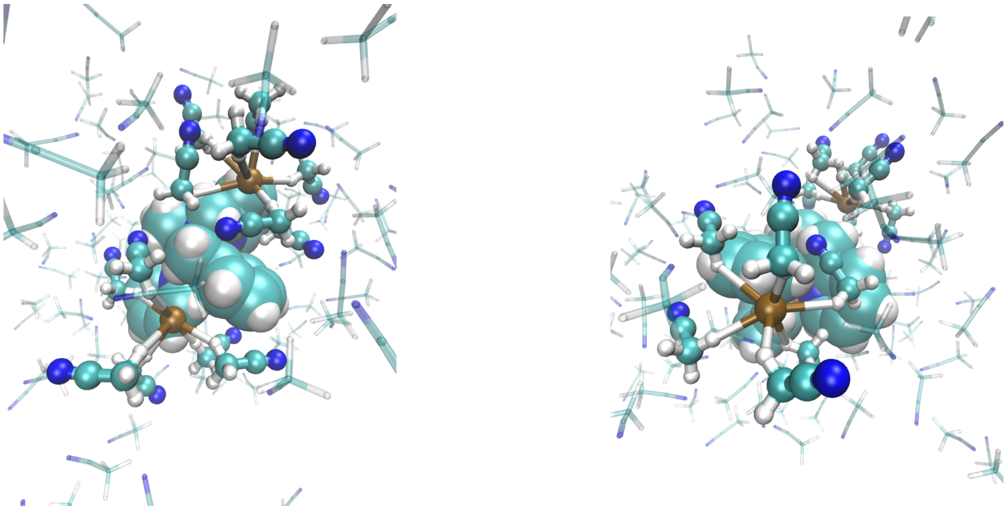

t = 32547.5 fs

t = 71000.0 fs

Figure S8 Snapshots from the LS trajectory illustrating the first solvation shell of the Cl$^-$ counterions: a CPK representation is used to draw the anions and the ACN molecules in their first solvation shell, and the shortest Cl$^-$-H$_{\mathrm{ACN}}$ bonds are drawn. LS [Fe(tpen)]$^{2+}$ is drawn with a van der Waals representation, and the remaining ACN molecules are shown in a transparent licorice representation. At t = 32547.5 fs, the Fe-Cl distances are 5.632 and 6.128 Å for the anions in the foreground and in the background, respectively; at t = 71000.0 fs, these distances become 7.586 and 5.871 Å for the anions in the foreground and in the background, respectively.

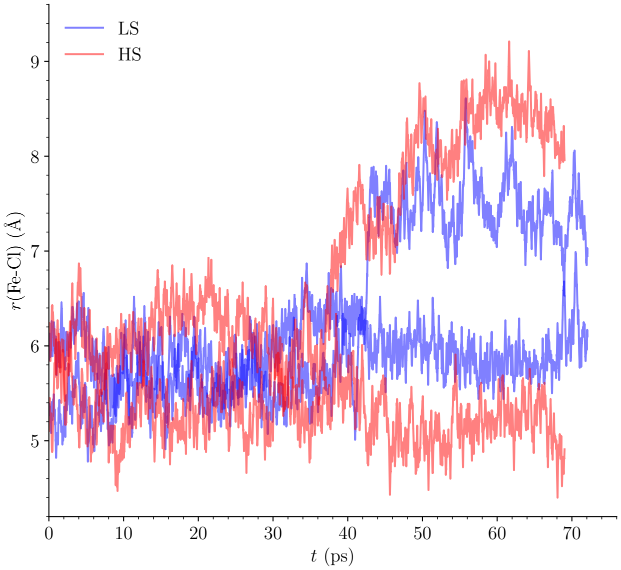

Figure S9 Time dependence of the Fe-Cl distances for [Fe(tpen)]$^{2+}$ in the LS and in the HS state.

2 Vibrational properties

2.1 Calculated 310 K Infrared spectrum of the acetotrinile solvent

The 310 K IR spectra of the acetonitrile solvent calculated for $[\mathrm{Fe(tpen)}]^{2+}$ in the LS and HS states are shown in Figure S10: the spectrum does not change with the spin state of $[\mathrm{Fe(tpen)}]^{2+}$.

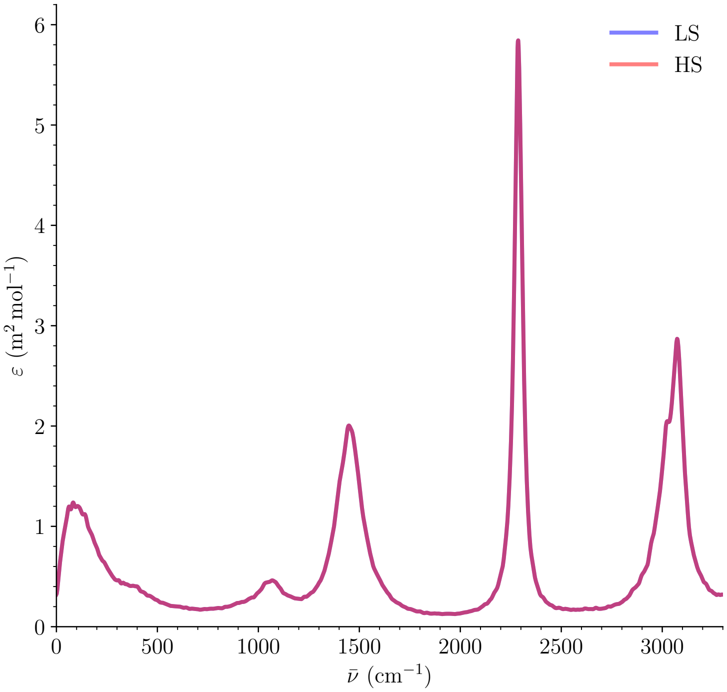

Figure S10 Calculated 310 K IR spectra of acetonitrile for $[\mathrm{Fe(tpen)}]^{2+}$ in the LS and HS state.

2.2 Infrared spectra $[\mathrm{Fe(tpen)}]^{2+}$ in the LS and HS states

Figure S11 allows the comparison between the IR spectra of $[\mathrm{Fe(tpen)}]\mathrm{Cl}_2$ and $[\mathrm{Fe(tpen)}]^{2+}$ in ACN. The spectrum of $[\mathrm{Fe(tpen)}]\mathrm{Cl}_2$ in given spin state has been determined by subtracting from the IR spectrum of the whole system the contribution of the solvent. For the system in either spin state, there exist small differences between the spectra of $[\mathrm{Fe(tpen)}]\mathrm{Cl}_2$ and $[\mathrm{Fe(tpen)}]^{2+}$ which is due to the fact that the spectrum $[\mathrm{Fe(tpen)}]\mathrm{Cl}_2$ includes the contributions of the Cl^- anions with their fluctuating charge distributions as well as the added solute-

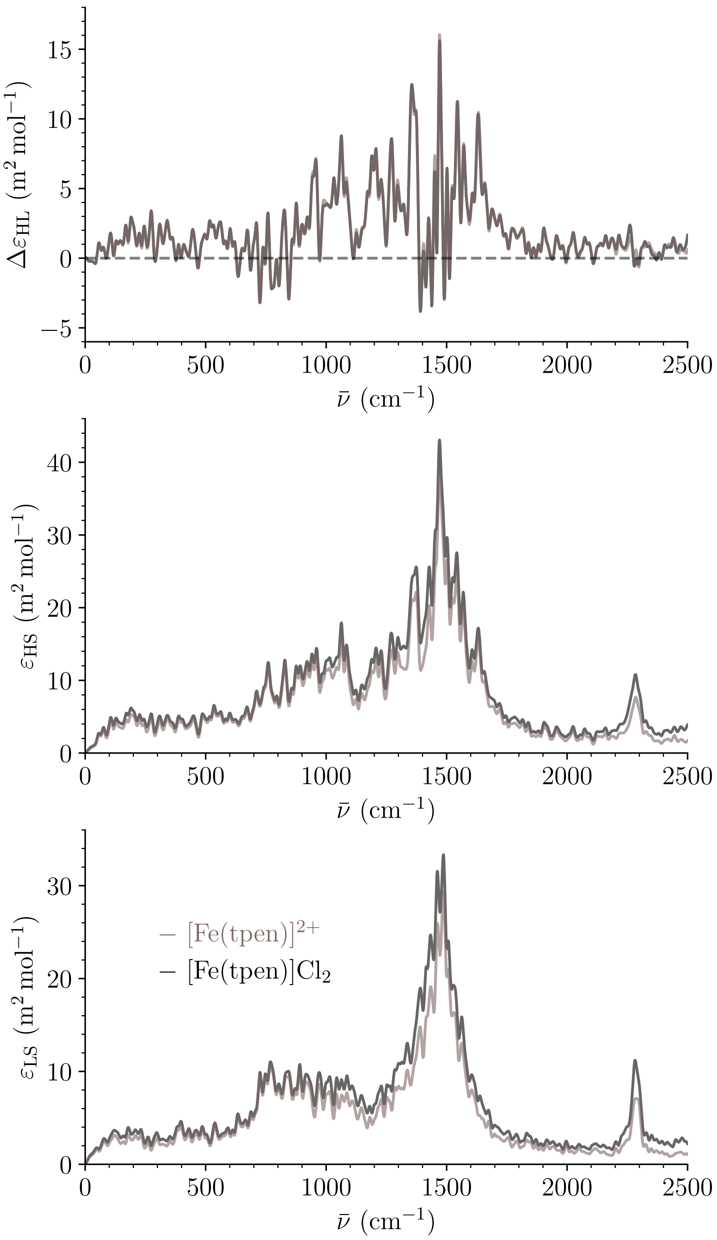

Figure S11 Comparison between the calculated 310 K IR spectra of $[\mathrm{Fe(tpen)}]\mathrm{Cl_2}$ and $[\mathrm{Fe(tpen)}]^{2+}$ in acetonirile: LS (bottom) and HS (middle) IR spectra, and corresponding HS-LS difference curves (top; resolution of the ACFs: 512 time steps).

solute and solute-solvent intermolecular contributions. These additional contributions show a vanishing dependence on the spin state since they cancel out when the difference spectrum is calculated. Figure S11 indeed shows that the HS-LS difference spectra of $[\mathrm{Fe(tpen)}]\mathrm{Cl_2}$ and $[\mathrm{Fe(tpen)}]^{2+}$ match each other almost perfectly.